was removed from UCR-20GaGeS-TAEA in the same experiment.

Ion exchange with NH_4^+ followed by calcination makes it possible to remove extra-framework species at temperatures as low as 100°C. For NH_4^+-exchanged UCR-20GaGeS-TAEA, a thermogravimetric analysis showed that the weight loss of 17.2% occurred between 80° and 150°C, which is much less than the temperature range needed for the direct calcination of the as-synthesized amine-containing sample (300° to 360°C). An x-ray powder diffraction shows that the sample remains highly crystalline after the calcination of the NH_4^+-exchanged sample at 180°C under argon atmosphere (fig. S2).

In addition to NH_4^+, these materials undergo ion exchange with many mono- and divalent metal cations. For example, upon exchange with Cs^+ ions, the percentages of C, H, and N in UCR-20GaGeS-TAEA were dramatically reduced (*20*). Yet, like the original sample, the exchanged sample remains highly crystalline. The Cs^+-exchanged UCR-20GaGeS-TAEA exhibits the type I isotherm characteristic of a microporous solid (Fig. 4). This sample has a high Langmuir surface area of 807 m^2/g and a micropore volume of 0.23 cm^3/g, despite the presence of much heavier elements (Cs, Ga, Ge, and S), as compared to the elements present in aluminosilicate zeolites. The median pore diameter calculated with the Horvath-Kawazoe method is 9.5 Å, 14% larger than that for Molecular Sieve Type 13X (8.2 Å) determined under the same experimental conditions.

These sulfides are also strongly photoluminescent and can be excited with wavelengths from 360 to 420 nm. The emission maximum occurs in the range from 460 to 508 nm (Fig. 5). For example, UCR-20GaGeS-TAEA strongly luminesces at 480 nm when excited at 370 nm. The general trend is that materials with heavier elements are excited and luminesce at a longer wavelength.

References and Notes

1. M. E. Davis, *Nature* **417**, 813 (2002).
2. Ch. Baerlocher, W. M. Meier, D. H. Olson, *Atlas of Zeolite Framework Types* (Elsevier, Amsterdam, 2001).
3. A. Corma, M. J. Diaz-Cabanas, J. Martinez-Triguero, F. Rey, J. Rius, *Nature* **418**, 514 (2002).
4. A. K. Cheetham, G. Ferey, T. Loiseau, *Angew. Chem. Int. Ed.* **38**, 3268 (1999).
5. R. L. Bedard, S. T. Wilson, L. D. Vail, J. M. Bennett, E. M. Flanigen, in *Zeolites: Facts, Figures, Future. Proceedings of the 8th International Zeolite Conference*, P. A. Jacobs, R. A. van Santen, Eds. (Elsevier, Amsterdam, 1989), pp. 375–387.
6. C. L. Cahill, J. B. Parise, *J. Chem. Soc. Dalton Trans.* **2000**, 1475 (2000).
7. S. Dhingra, M. G. Kanatzidis, *Science* **258**, 1769 (1992).
8. R. W. J. Scott, M. J. MacLachlan, G. A. Ozin, *Curr. Opin. Solid State Mater. Sci.* **4**, 113 (1999).
9. H. Li, A. Laine, M. O'Keeffe, O. M. Yaghi, *Science* **283**, 1145 (1999).
10. H. Ahari, A. Lough, S. Petrov, G. A. Ozin, R. L. Bedard, *J. Mater. Chem.* **9**, 1263 (1999).
11. O. M. Yaghi, Z. Sun, D. A. Richardson, T. L. Groy, *J. Am. Chem. Soc.* **116**, 807 (1994).
12. K. Tan, A. Darovsky, J. B. Parise, *J. Am. Chem. Soc.* **117**, 7039 (1995).
13. C. L. Bowes *et al.*, *Chem. Mater.* **8**, 2147 (1996).
14. E. M. Flanigen, in *Introduction to Zeolite Science and Practice*, H. van Bekkum, E. M. Flanigen, J. C. Jansen, Eds. (Elsevier, New York, 1991), pp. 13–34.
15. P. Feng, X. Bu, G. D. Stucky, *Nature* **388**, 735 (1997).
16. X. Bu, P. Feng, G. D. Stucky, *Science* **278**, 2080 (1997).
17. X. Bu, N. Zheng, Y. Li, P. Feng, *J. Am. Chem. Soc.* **124**, 12646 (2002).
18. C. Wang, X. Bu, N. Zheng, P. Feng, *J. Am. Chem. Soc.* **124**, 10268 (2002).
19. An example of a typical synthesis condition with the preparation of UCR-20GaGeS-TAEA is as follows. Gallium metal (82.7 mg), germanium oxide (109.1 mg), sulfur (222.1 mg), and tris(2-aminoethyl)amine (2.1719 g) were mixed in a Teflon-lined stainless steel autoclave for ~20 min. The vessel was then sealed and heated at 190°C for 6 days. The autoclave was subsequently cooled to room temperature. Transparent, pale yellow crystals were obtained with a yield of ~67%.
20. Materials and methods, results of the elemental analysis, details of the thin-film structure, and x-ray powder diffraction data are available on *Science* Online. Crystallographic data (excluding structure factors) have been deposited with the Cambridge Crystallographic Data Center (CCDC) as supplementary publications CCDC 197105 through 197126 and CCDC 197207 through 197214.
21. M. O'Keeffe, M. Eddaoudi, H. Li, T. Reineke, O. M. Yaghi, *J. Solid State Chem.* **152**, 3 (2002).
22. G. O. Brunner, W. M. Meier, *Nature* **337**, 146 (1989).
23. H. Li, J. Kim, T. L. Groy, M. O'Keeffe, O. M. Yaghi, *J. Am. Chem. Soc.* **123**, 4867 (2001).
24. C. Wang *et al.*, *J. Am. Chem. Soc.* **123**, 11506 (2001).

25. Supported by NSF (grant CHE-0213310) and the Air Force Office of Scientific Research (for a grant to purchase an x-ray powder diffractometer). We thank H. Luo, S. Li, and Y. Yan for their assistance with adsorption measurements.

Supporting Online Material

www.sciencemag.org/cgi/content/full/298/5602/2366/DC1
Materials and Methods
Figs. S1 and S2
Table S1

23 September 2002; accepted 12 November 2002

Mass-Independent Sulfur of Inclusions in Diamond and Sulfur Recycling on Early Earth

J. Farquhar,[1] B. A. Wing,[1] K. D. McKeegan,[2] J. W. Harris,[3] P. Cartigny,[4] M. H. Thiemens[5]

Populations of sulfide inclusions in diamonds from the Orapa kimberlite pipe in the Kaapvaal-Zimbabwe craton, Botswana, preserve mass-independent sulfur isotope fractionations. The data indicate that material was transferred from the atmosphere to the mantle in the Archean. The data also imply that sulfur is not well mixed in the diamond source regions, allowing for reconstruction of the Archean sulfur cycle and possibly offering insight into the nature of mantle convection through time.

An understanding of the nature of the source materials for diamonds would provide important insights into large-scale geophysical processes. For example, elemental and isotopic data have been used to argue that diamonds and their inclusions are relics of subducted crustal materials (*1–9*), but alternate explanations such as mantle fractionation processes or relict primordial heterogeneity are plausible (*10–15*). Here we report mass-independently fractionated {anomalous $\Delta^{33}S = \delta^{33}S - 1000 \times [(1 + \delta^{34}S/1000)^{0.515} - 1]$} (*16*) sulfur isotope compositions for syngenetic sulfide inclusions in diamond from the Orapa kimberlite pipe, Kaapvaal-Zimbabwe craton, Botswana. We also discuss the implications of $\Delta^{33}S$ as an almost perfect tracer of the exchange between Earth's geochemical reservoirs because of its exclusive origin through atmospheric photochemistry and its preservation through subsequent mass-dependent fractionation processes.

The Orapa kimberlite pipe is located within the Magondi belt, a region of thick (150 to 225 km) crust along the western margin of the Kaapvaal-Zimbabwe craton, which is considered to be the surface manifestation of the Proterozoic reactivation of the Kaapvaal-Zimbabwe craton (*17–19*). Diamonds from Orapa are predominantly eclogite types and have a wide range of $\delta^{13}C$ values [(–26 to –3 per mil (‰)], $\delta^{15}N$ values (–10 to +6‰), nitrogen contents [(8 to 3450 parts per million (ppm)], and nitrogen aggregation states (a 0 to 95% degree of association) (*1*, *12*, *20*). Silicate and sulfide inclusions from these diamonds have at least two distinct ages (*1*, *19*): an Archean population of 2.9 Ga and a Proterozoic population of 1.0 billion years ago (Ga) (*1*, *19*). The sulfide inclusions also have

[1]Earth System Science Interdisciplinary Center and Department of Geology, University of Maryland, College Park, MD 20742, USA. [2]Department of Earth and Space Sciences, University of California, Los Angeles, CA 90095, USA. [3]Division of Earth Sciences, Gregory Building, University of Glasgow, Glasgow, G12 8QQ, UK. [4]Laboratoire de Géochimie des Isotopes Stables, Université Paris VII, Institut de Physique du Globe de Paris, 75252 Paris Cedex 05, France. [5]Department of Chemistry and Biochemistry, University of California, San Diego, La Jolla, CA 92093, USA.

a wide range of $\delta^{34}S$ (–11 to +9.5‰) that may relate to recycling of sedimentary materials (*2*, *3*, *11*).

We extracted sulfide inclusions from 12 Orapa diamonds for sulfur isotope analysis. These inclusions consist of finely exsolved monosulfide solid solution with micron-scale Ni-rich and Cu-rich exsolution features. One of the host diamonds (ORJF2) contained silicate inclusions of eclogite-type (e-type) garnets and clinopyroxene. The other 11 diamonds contained only sulfide inclusions. The sulfide inclusions (table S1) have low Ni contents and also contain significant amounts of Cu and Co, suggesting an e-type affinity (*21*). Data for Orapa sulfides are comparable but have a narrower range than previous measurements (*22*).

The sulfur isotope compositions of 23 individual inclusions (45 spot analyses) were measured by secondary ion mass spectrometry with the University of California, Los Angeles Cameca IMS 1270 ion microprobe (table S2). Multiple Faraday cup detectors were used for simultaneous measurement of $^{32}S^-$, $^{33}S^-$, and $^{34}S^-$ ion beams (*23*). Two-sigma uncertainties are ±0.12‰ for single $\Delta^{33}S$ analyses and ±1.4‰ for $\delta^{34}S$ spot analyses. Our $\delta^{34}S$ values yield a smaller range (–1.4 to 2.6‰) than has been previously observed for Orapa sulfides (*2*, *3*). The smaller range for both the $\delta^{34}S$ and the Ni content of our data relative to that presented by prior studies suggests that we have analyzed a subset of the Orapa sulfide population. With one possible exception (ORJF2G4), $\Delta^{33}S$ and $\delta^{34}S$ analyses of individual sulfide grains from the same diamond are indistinguishable from one another within our analytical uncertainties. On the basis of homogeneous $\Delta^{33}S$, we grouped inclusions into populations that are defined on the basis of the diamond in which they are found (Fig. 1). The $\Delta^{33}S$ values of different inclusion populations extend from –0.11 to 0.61‰, with $\Delta^{33}S$ anomalies resolvable at the 2σ level from $\Delta^{33}S$ = 0 in 4 of the 12 diamonds.

The lack of resolvable $\Delta^{33}S$ variability among inclusions from a single diamond suggests that the source of sulfur for each population of inclusions (i.e., from an individual diamond) was well mixed and characteristic of the immediate region in which the diamond formed. The variations in $\Delta^{33}S$ among sulfide grains from different diamonds imply that heterogeneity does exist, but at a scale larger than that sampled by any single diamond. The present data are insufficient to determine whether $\Delta^{33}S$ variability is coupled to other chemical and isotopic heterogeneity (*1*, *12*, *20*). C and N in diamonds and Ni in diamond sulfide inclusions might have a different source than sulfur and may be uncoupled.

Classical thermodynamic, kinetic, and diffusion-controlled fractionation processes all produce highly correlated relations between $\delta^{33}S$ and $\delta^{34}S$ such that $\Delta^{33}S$ typically varies by less than 0.01‰ for every 1‰ variation of $\delta^{34}S$. Although minor variations of $\Delta^{33}S$ can be generated by different types of mass-dependent fractionation processes (*24*–*27*), these processes cannot account for the larger magnitude of the observed anomalous $\Delta^{33}S$ of sulfide inclusions and its lack of dependence on variations for $\delta^{34}S$ (Fig. 1). This rules out the possibility that mass-dependent fractionation processes in the mantle could have caused the $\Delta^{33}S$ anomalies.

We do not favor interpreting the anomalous $\Delta^{33}S$ values as primordial heterogeneities inherited from diverse sources during accretion of Earth. Although nonzero $\Delta^{33}S$ values have been observed in some rare components of meteorites (*28*–*32*), sequential acid extracts and bulk extracts of sulfide sulfur and sulfate sulfur from carbonaceous chondrites, enstatite chondrites, ordinary chondrites, iron meteorites, and ureilites have indicated that $\Delta^{33}S$ is homogeneous and has a range of values between –0.01 and +0.04‰ (*28*, *29*, *33*, *34*).

Recently, large positive and negative $\Delta^{33}S$ values up to a few per mil have been observed in Archean crustal and sedimentary rocks (*16*). The origin of these anomalous $\Delta^{33}S$ values is attributed to atmospheric photochemistry involving sulfur dioxide in a primitive atmosphere with reduced oxygen and ozone and increased ultraviolet transparency (*16*, *35*). When the data for Archean $\Delta^{33}S$ are plotted versus $\delta^{34}S$ (Fig. 2), they define an area that includes the observed data for sulfide inclusions from Orapa diamonds. The $\Delta^{33}S$ signature observed in some sulfide inclusions from Orapa diamonds is consistent with the recycling of this surface sulfur reservoir.

The preservation of anomalous sulfur in these inclusions allows us to place constraints on the coupling between Archean mantle, crust, and atmosphere. The mean $\Delta^{33}S$ of peridotite xenoliths from Kilbourne Hole is taken as an estimate for the mantle composition (0.03 ± 0.04‰ 2σ). Monte Carlo resampling of the mean $\Delta^{33}S$ value for Archean sulfide (*16*) yields a $\Delta^{33}S$ of 0.51 ± 0.30‰ for the average Archean crustal sulfide composition. The experimental determination of the isotopic composition of elemental sulfur produced by photolysis of sulfur dioxide with 193-nm radiation has $\Delta^{33}S$ = 65 ± 4‰ (*35*).

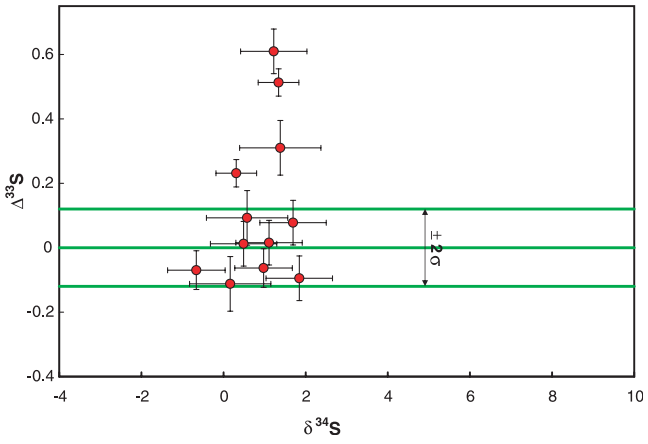

Fig. 1. Plot of $\Delta^{33}S$ and $\delta^{34}S$ of inclusion populations from individual diamonds from the Orapa kimberlite pipe (red points). Two-sigma mean uncertainty estimates for each inclusion population are presented assuming that they are given by 0.12‰ × $n^{-1/2}$ and 1.4‰ × $n^{-1/2}$, respectively, where n is the number of points analyzed and 0.12 and 1.4‰ are estimates of the 2σuncertainty made on the basis of long-term reproducibility of the working standard (CAR 123). The shaded region centered at $\Delta^{33}S$ = 0 and extending from +0.12 to –0.12‰ is assumed to represent the mass-dependent field. Four points are distinguished from this field and are interpreted to be mass-independent. For reasons that are not known, the $\delta^{34}S$ values of different inclusions define a smaller range than observed previously (*2*, *3*).

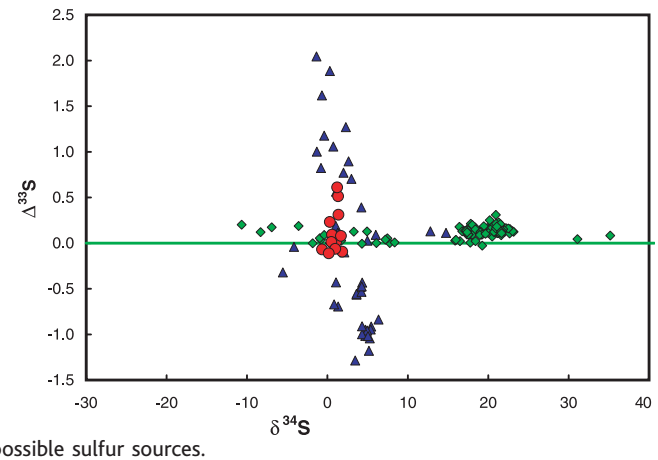

Fig. 2. Plot of $\Delta^{33}S$ and $\delta^{34}S$ of inclusion populations from individual diamonds from the Orapa kimberlite pipe (red circles), with the same aspect ratio as Fig. 1 that also includes data for Archean samples (blue triangles) and data for samples younger than 2.45 Ga (green diamonds) that were reported in (*16*) and (*38*) as well as additional mass-dependent data (table S3). This plot allows comparison of the sulfide inclusion data from Orapa diamonds with data from possible sulfur sources.

Because the $\Delta^{33}S$ values of the anomalous inclusions are directly comparable to those of the average Archean crustal sulfide, our data indicate that all of the sulfur in these inclusions may represent recycled but undiluted crustal sulfur. Material balance also dictates that up to 1% of the sulfur in these inclusions was processed through the Archean atmosphere. This estimate is a lower limit because we assumed that the maximum mass-independent fractionation that was observed in the photolysis experiments (*35*) is applicable to the Archean atmosphere. Our detection limits of ±0.12‰ would also allow for up to 25% of the sulfur in the mass-dependent diamonds to derive from a surface sulfide reservoir with a $\Delta^{33}S$ of 0.51‰. The heterogeneous $\Delta^{33}S$ may reflect different proportions of surface-derived sulfur, or it may reflect variable $\Delta^{33}S$ of the recycled component.

A conceptual model of the sulfur cycle indicated by the data (Fig. 3) starts with a volcanic source releasing mass-dependent sulfur-bearing gases into the atmosphere. Photolysis of these gases produces a photochemical fractionation of sulfur between elemental and oxidized forms, each with a unique and anomalous $\Delta^{33}S$. The anomalous sulfur is transferred to surface reservoirs through atmospheric deposition and the elemental sulfur species are converted to sulfide (possibly by microbial activity). After sedimentation, lithification, and metamorphism, the anomalous sulfur is recycled into the mantle. Evidence for these connections is only preserved, however, because the sulfur was encased in diamond and ultimately transported back to Earth's surface. Mass balance in the sulfur cycle requires an equivalent flux of a ^{33}S-depleted ($\Delta^{33}S < 0$) component or a net decrease of $\Delta^{33}S$ in one or more of the exospheric sulfur reservoirs, or some combination of the two. The sign of the anomalous $\Delta^{33}S$ in our four diamonds is positive, like both the elemental sulfur produced by 193-nm photolysis and most of the measured Archean sulfides (*16*, *35*), and unlike the sulfate produced in the photolysis experiments and observed in Archean samples (*16*, *35*). If our samples are representative, the coincidence of positive $\Delta^{33}S$ for sulfide inclusions and average Archean sulfide suggests that the sulfur in the inclusions is predominantly derived from a sedimentary sulfide component that was subducted to the source regions of the Orapa diamonds. Given that measurements of $\Delta^{33}S$ from Archean barites are uniformly negative (*16*) and that measurements of $\Delta^{33}S$ from rocks with clear oceanic association also carry this signature, accumulation of ^{33}S in the Archean ocean might be sufficient to close the ^{33}S mass balance.

Transfer of the negative $\Delta^{33}S$ signature from the oceanic sulfate reservoir, through sulfate reduction during basalt alteration and subsequent subduction of the altered basalt, may provide a mechanism, however, that satisfies mass balance constraints. Although a subducted ^{33}S-depleted basaltic component is not mandated by our observations, the recognition of potential deep-mantle lithospheric graveyards (*36*, *37*) leads to the possibility that these regions contain the missing ^{33}S-depleted component. The presence of ^{33}S-enriched mantle domains with sedimentary affinities and ^{33}S-depleted mantle domains with oceanic affinities remains to be tested. These sulfur isotope data constitute a new type of isotope tracer that allows a reconstruction of the Archean sulfur cycle, and they indicate an interconnected global geochemical sulfur cycle extending from the atmosphere to the mantle on ancient Earth.

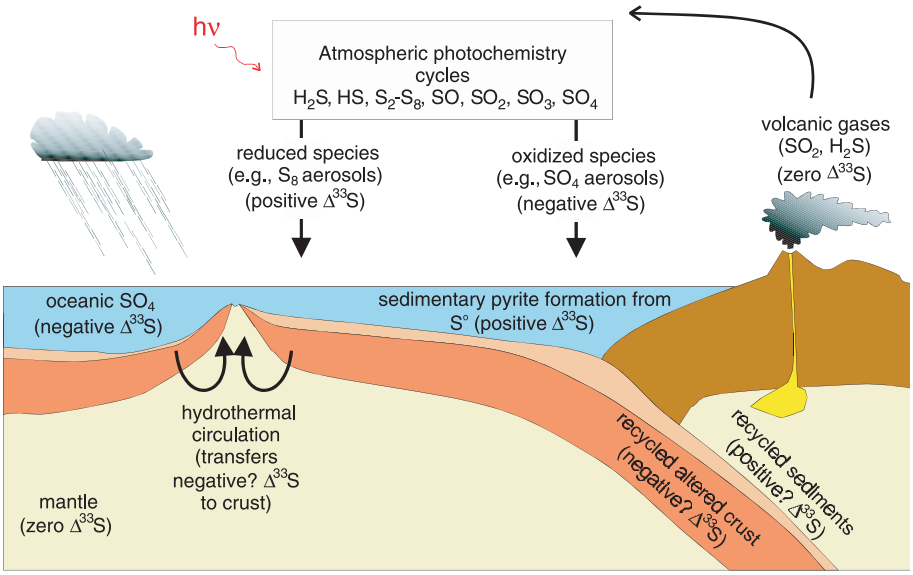

Fig. 3. Components of the geochemical sulfur cycle that are indicated by the data for sulfide inclusions from Orapa. Anomalous $\Delta^{33}S$ of sulfide inclusions in diamond was produced when sulfur dioxide of volcanogenic origin was photodissociated in the Archean atmosphere by deep ultraviolet radiation. This signature was transferred first to sedimentary sulfide and subsequently to the mantle by subduction-related processes. Diamond formation in the mantle encapsulated the sulfides and preserved them until the point at which they were transported to Earth's surface. Observations of negative $\Delta^{33}S$ for Archean barite indicate that the oceanic reservoir had negative $\Delta^{33}S$. Hydrothermal reduction of oceanic sulfate with negative $\Delta^{33}S$ would transfer this signature to the hydrothermally altered products. Recycling of altered crust to the mantle may therefore close the sulfur balance required by the sulfide inclusion data. Sulfides in shales appear to be the most substantial repository for $\Delta^{33}S$-enriched sulfur (*16*).

References and Notes

1. S. B. Shirey *et al.*, *Science* **297**, 1683 (2002).
2. M. Chaussidon, F. Albarede, S. M. F. Sheppard, *Nature* **330**, 242 (1987).
3. C. S. Eldridge, W. Compston, I. S. Williams, J. W. Harris, J. W. Bristow, *Nature* **353**, 649 (1991).
4. C. B. Smith *et al.*, *Geochim. Cosmochim. Acta* **55**, 2579 (1991).
5. R. L. Rudnick, C. S. Eldridge, G. P. Bulanova, *Geology* **21**, 13 (1993).
6. S. Aulbach, T. Stachel, K. S. Viljoen, G. P. Brey, J. W. Harris, *Contrib. Mineral. Petrol.* **143**, 56 (2002).
7. T. Stachel, J. W. Harris, S. Aulbach, P. Deines, *Contrib. Mineral. Petrol.* **142**, 465 (2002).
8. S. H. Richardson, S. B. Shirey, J. W. Harris, R. W. Carlson, *Earth Planet. Sci. Lett.* **191**, 257 (2001).
9. N. V. Sobolev, E. M. Galimov, I. N. Ivanovskaia, E. S. Efimova, *Dokl. Akad. Nauk SSSR* **249**, 1217 (1979).
10. P. Deines, J. W. Harris, J. J. Gurney, *Geochim. Cosmochim. Acta* **51**, 1227 (1987).
11. J. J. Gurney, *Nature* **353**, 601 (1991).
12. P. Deines, J. W. Harris, J. J. Gurney, *Geochim. Cosmochim. Acta* **57**, 2781 (1993).
13. P. Cartigny, J. W. Harris, M. Javoy, *Science* **280**, 1421 (1998).
14. P. Cartigny, J. W. Harris, D. Phillips, M. Girard, M. Javoy, *Chem. Geol.* **147**, 147 (1998).
15. S. E. Haggerty, *Science* **285**, 851 (1999).
16. J. Farquhar, H. M. Bao, M. Thiemens, *Science* **289**, 756 (2000).
17. T. K. Nguuri *et al.*, *Geophys. Res. Lett.* **28**, 2501 (2001).
18. D. E. James, M. J. Fouch, J. C. VanDecar, S. van der Lee, *Geophys. Res. Lett.* **28**, 2485 (2001).
19. S. B. Shirey *et al.*, *Geophys. Res. Lett.* **28**, 2509 (2001).
20. P. Cartigny, J. W. Harris, M. Javoy, in *The 7th International Kimberlite Conference Proceedings, The J. B. Dawson Volume*, J. L. Gurney, J. J. Gurney, M. D. Pascor, S. H. Richardson, Eds. (Red Roof Design, Cape Town, South Africa, 1999), pp. 117–124.
21. G. P. Bulanova, W. L. Griffin, C. G. Ryan, O. Y. Shestakova, S. J. Barnes, *Contrib. Mineral. Petrol.* **124**, 111 (1996).
22. P. Deines, J. W. Harris, *Geochim. Cosmochim. Acta* **59**, 3173 (1995).
23. Materials and methods are available as supporting material on *Science* Online.
24. J. R. Hulston, H. G. Thode, *J. Geophys. Res.* **70**, 3475 (1965).
25. Y. Matsuhisa, J. R. Goldsmith, R. N. Clayton, *Geochim. Cosmochim. Acta* **42**, 173 (1978).
26. E. D. Young, A. Galy, H. Nagahara, *Geochim. Cosmochim. Acta* **66**, 1095 (2002).
27. M. F. Miller, *Geochim. Cosmochim. Acta* **66**, 1881 (2002).
28. X. Gao, M. H. Thiemens, *Geochim. Cosmochim. Acta* **55**, 2671 (1991).
29. ———, *Geochim. Cosmochim. Acta* **57**, 3159 (1993).
30. G. W. Cooper, M. H. Thiemens, T. L. Jackson, S. Chang, *Science* **277**, 1072 (1997).
31. C. E. Rees, H. G. Thode, *Geochim. Cosmochim. Acta* **41**, 1679 (1977).

32. J. R. Hulston, H. G. Thode, *J. Geophys. Res.* **70**, 4435 (1965).
33. X. Gao, M. H. Thiemens, *Geochim. Cosmochim. Acta* **57**, 3171 (1993).
34. J. Farquhar, T. L. Jackson, M. H. Thiemens, *Geochim. Cosmochim. Acta* **64**, 1819 (2000).
35. J. Farquhar, J. Savarino, S. Airieau, M. H. Thiemens, *J. Geophys. Res. Planets* **106**, 32829 (2001).
36. F. Albarede, R. D. van der Hilst, *Eos* **80**, 535 (1999).
37. R. D. van der Hilst, H. Karason, *Science* **283**, 1885 (1999).
38. D. Heymann *et al.*, *Geochim. Cosmochim. Acta* **62**, 173 (1998).
39. We acknowledge and thank DeBeers for providing diamonds; M. Chaussidon for sulfur isotope standards; A. D. Brandon for providing peridotite samples from Kilbourne Hole; A. Paytan for making her data available to us; NSF, NASA, and American Chemical Society for support to J.F. and B.A.W.; and the NASA Astrobiology program for supporting sulfur isotope studies at UCLA and University of Maryland, College Park. The UCLA ion microprobe facility is partially supported by a grant from the NSF Instrumentation and Facilities program. J.F. acknowledges editing and insights of L.J. Tuit.

Supporting Online Material
www.sciencemag.org/cgi/content/full/298/5602/2369/DC1
Materials and Methods
Tables S1 to S3

20 September 2002; accepted 11 November 2002

Calibration of Sulfate Levels in the Archean Ocean

Kirsten S. Habicht,[1] Michael Gade,[1] Bo Thamdrup,[1] Peter Berg,[2] Donald E. Canfield[1]*

The size of the marine sulfate reservoir has grown through Earth's history, reflecting the accumulation of oxygen into the atmosphere. Sulfur isotope fractionation experiments on marine and freshwater sulfate reducers, together with the isotope record, imply that oceanic Archean sulfate concentrations were <200 μM, which is less than one-hundredth of present marine sulfate levels and one-fifth of what was previously thought. Such low sulfate concentrations were maintained by volcanic outgassing of SO_2 gas, and severely suppressed sulfate reduction rates allowed for a carbon cycle dominated by methanogenesis.

It is thought that the Archean Earth had low atmospheric oxygen concentrations (*1*), low oceanic sulfate concentrations (*2*), and elevated atmospheric concentrations of methane, contributing to possible greenhouse warming of Earth's surface (*3*). The biogeochemistries of these elements are linked, in that low atmospheric oxygen levels suppress the oxidative weathering of sulfides and the delivery of sulfate to the oceans, contributing to the low sulfate concentrations (*2*). Low sulfate levels could have inhibited sulfate reduction, enhancing methane production (*2*, *4*).

This reconstruction depends on our ability to extract reliable sulfate concentration information from the isotope record of sulfide and sulfate through time. The isotope record reveals small fractionations of generally <10 per mil (‰) between sulfates and sedimentary sulfides before 2.5 to 2.7 billion years ago (Ga) (*2*). The few available pure culture studies suggest that fractionations become suppressed at a sulfate concentration around 1 mM (*5*, *6*). Current models link reduced fractionations at low sulfate concentration to a limitation of sulfate exchange across the cell membrane (*6*). In this case, most of the sulfate entering the cell becomes reduced, and even with substantial internal enzymatic fractionations, minimal net fractionation is expressed. Sulfate limitation also reduces sulfate reduction rates, with half-saturation constants (k_m) values for marine strains of 70 and 200 μM (*7*, *8*) and for freshwater strains, 5 to 30 μM (*7*). If similar sulfate concentrations limit both fractionation and sulfate reduction rate, then sulfate reducers should maintain substantial fractionation at sulfate concentrations considerably less than 1 mM.

In continuous culture, we explored the fractionations at millimolar and submillimolar sulfate concentrations by *Archaeoglobus fulgidus* grown on lactate at its optimal growth for temperature of 80°C. *A. fulgidus* is an archaeon and was chosen to represent possible early sulfate reducers from hydrothermal settings. We also examined natural populations of sulfate reducers from a coastal marine sediment (natural sulfate concentration, 20 mM) and a freshwater lake sediment (natural sulfate concentration, 300 μM). Freshwater sulfate reducers are especially adapted to low sulfate concentrations (*9*) and could reflect the behavior of possible early low sulfate–adapted organisms, whereas marine sulfate reducers are adapted to high seawater salinities. In the natural population experiments, sediment was incubated at 17°C in a rapidly recirculating flow-through plug reactor (*10*) with lactate (1 mM) as the organic substrate (*11*).

All three different microbial populations produced high fractionations (*11*) of up to 32‰ with 200 μM or greater sulfate (Fig. 1). The average fractionation for sulfate between 200 and 1000 μM was 22.6 ± 10.3‰, which is similar to the average for pure bacterial cultures (*6*) (18 ± 10‰) and natural populations (*6*) (28 ± 6‰) of sulfate reducers utilizing 20 mM or greater sulfate. By contrast, fractionations were consistently less than 6‰ (an average of 0.7 ± 5.2‰) with sulfate concentrations less than 50 μM. Thus, sulfate substantially limited fractionation up to a concentration somewhere between 50 μM and around 200 μM. This is also the concentration range where sulfate limits rates of sulfate reduction (*8*, *9*).

The isotopic composition of sedimentary sulfides will, in addition to the bacterial fractionation, depend on the extent to which sulfides form in a zone of sulfate depletion (*6*,

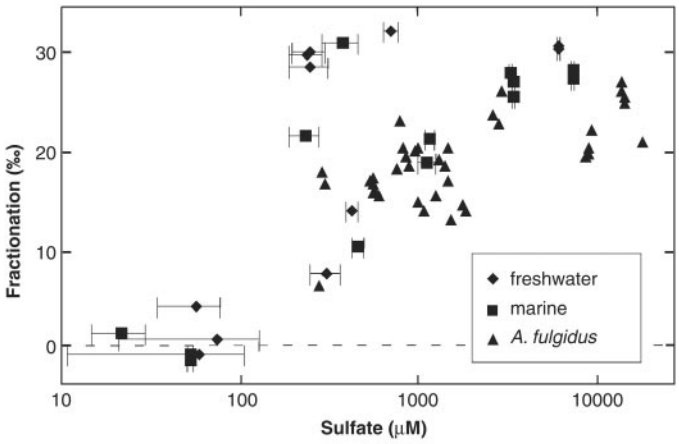

Fig. 1. Isotope fractionation as a function of sulfate concentration for freshwater (diamonds) and marine (squares) natural populations of sulfate reducers and for the hyperthermophile *A. fulgidus* (triangles). For the freshwater and marine populations, horizontal bars plot the range of sulfate concentrations within the reactor, with the higher concentration entering the reactor, and the low concentration exiting the reactor. The symbols are positioned on the bars at the average concentration in the reactor.

[1]Danish Center for Earth System Science and Institute of Biology, University of Southern Denmark, Campusvej 55, DK-5230, Odense M, Denmark. [2]Department of Environmental Sciences, Clark Hall, University of Virginia, VA 22903, USA.

*To whom correspondence should be addressed.